

RESEARCH

Open Access



Thalidomide attenuates radiation-induced apoptosis and pro-inflammatory cytokine secretion in oral epithelial cells by promoting LZTS3 expression

Leifeng Liang^{1†} , Mei Gan^{1†}, Huanshuo Miao^{2†}, Jinchi Liu³, Chunhong Liang⁴, Jinqiu Qin⁵, Kaian Ruan⁶, Haisheng Zhu¹, Jinghua Zhong^{7*} and Zhan Lin^{1*}

Abstract

Radiation-induced oral mucositis (RIOM) is a prevalent oral complication that occurs in individuals undergoing radiotherapy or radiation treatment for head and neck tumors. The presence of oral mucosal rupture and ulcerative lesions, which are the defining features of this condition, can significantly affect the quality of life of patients. Additionally, it can interfere with tumor therapy and contribute to an unfavorable prognosis. Current evidence suggests that cellular inflammation and programmed cell death are important factors in disease development. Moreover, thalidomide (THD) has been revealed to reduce the incidence and severity of RIOM in patients undergoing chemoradiotherapy for nasopharyngeal carcinoma. However, the mechanism through which THD improves RIOM remains unknown. This study aimed to investigate the role of LZTS3 in RIOM by analyzing various sequencing datasets and conducting knockdown and overexpression experiments. We used small interfering RNA transfection and LZTS3 overexpression, followed by validation through polymerase chain reaction, western blotting, flow cytometry, and enzyme-linked immunosorbent assay. In this study, we identified LZTS3 as a potential target for THD regulation in RIOM. Through a series of experiments, we confirmed that LZTS3 has the ability to inhibit the inflammatory response and apoptosis of cells. In addition, we also found that THD can regulate the expression of LZTS3 by upregulating, thereby affecting inflammatory response and apoptosis. We repeated these results in a live animal model. In summary, THD has the potential to reduce the occurrence of oral mucositis in patients by upregulating LZTS3 levels. These findings provide a promising avenue for future drug research and development to treat RIOM.

[†]Leifeng Liang, Mei Gan and Huanshuo Miao contributed equally to this work.

*Correspondence:
Jinghua Zhong
jinghuazhong2019@gmu.edu.cn
Zhan Lin
yulan.501@163.com

Full list of author information is available at the end of the article



© The Author(s) 2024. **Open Access** This article is licensed under a Creative Commons Attribution-NonCommercial-NoDerivatives 4.0 International License, which permits any non-commercial use, sharing, distribution and reproduction in any medium or format, as long as you give appropriate credit to the original author(s) and the source, provide a link to the Creative Commons licence, and indicate if you modified the licensed material. You do not have permission under this licence to share adapted material derived from this article or parts of it. The images or other third party material in this article are included in the article's Creative Commons licence, unless indicated otherwise in a credit line to the material. If material is not included in the article's Creative Commons licence and your intended use is not permitted by statutory regulation or exceeds the permitted use, you will need to obtain permission directly from the copyright holder. To view a copy of this licence, visit <http://creativecommons.org/licenses/by-nc-nd/4.0/>.

Keywords Thalidomide, LZTS3, Radiation-induced oral mucositis, Cellular inflammation, Programmed cell death, Inflammatory response, Apoptosis

Introduction

Radiation-induced oral mucositis (RIOM) is a prevalent issue among patients with head and neck tumors. This is primarily due to the significant toxicity associated with ionizing radiation therapy. In 1980, RIOM was first discovered as a side effect of radiation therapy (RT) in patients with cancer [1]. RIOM may manifest in more than 80% of patients undergoing radiotherapy for head and neck cancer, and it can affect approximately 100% of patients undergoing modified segmentation for head and neck cancer treatment. Among those who underwent RT for head and neck malignancies, 56% experienced severe RIOM, classified as grades 3 and 4 [2, 3]. Its primary characteristics comprise oral mucosa rupture and ulcerative lesion development, causing symptoms such as pain, swallowing difficulties, and a decreased quality of life [4]. The mechanism of RIOM is associated with radiation-induced cell death, and the immune system activation of the inflammatory cascade exacerbates this condition [5]. In RIOM, tissue damage persists between 7 and 98 days [2, 6], encompassing stages that include initiation, primary injury response, signal amplification, ulceration, and ultimately healing [7]. In the pre-ulcer stage, a significant release of inflammatory factors occurs, while cell apoptosis occurs in the epithelial and post-ulcer stages [8–10]. Thalidomide (THD), a synthetic compound derived from glutamate, inhibits nuclear factor κ B (NF- κ B) activation [11]. Owing to its anti-inflammatory properties, this synthetic derivative is used for leprosy treatment [12]. Recently, research has revealed the role of THD in treating various inflammatory and infectious conditions and other ailments, including multiple myeloma. Additionally, it is used for mucosal disorder treatment [13]. THD treatment improved RIOM outcomes in animal studies [14]. THD effectiveness and safety in preventing RIOM were confirmed in a previous multicenter randomized controlled clinical study [15]. However, the mechanism through which THD improves RIOM remains unknown.

This study determined the role of THD downstream LZTS3 by analyzing sequencing data sets. LZTS3 was first identified in 2005 and belongs to the leucine zipper tumor suppressors (LZTS) protein family [16]. But LZTS3 has not been reported to play a role in the regulation of RIOM. I conducted knockdown and overexpression experiments of LZTS3 in irradiated cell models, and discussed the effects of THD and radiation on LZTS3, as well as the role of LZTS3 in RIOM. Additionally, mouse models were developed to examine the protective mechanism of THD against RIOM, with a specific focus on

its effect on programmed cell death and immune system responses. These findings hold potential for the identification of therapeutic targets for RIOM patients.

Methods

Correlation between THD administration and radiation-induced oral mucositis in mice

Established guidelines for animal experiments were adhered to in this study, to ensure standard ARRIVE guidelines are followed. The protocol of this study was consistent with those of the national studies and adhered to council recommendations for the treatment and utilization of animals in laboratory settings. We acquired 4-week-old male C57BL/6J mice from the Animal Laboratory Center at Guangxi Medical University, housing them in a specific pathogen-free environment. After a 1-week acclimatization period, we randomly assigned 25 mice to five groups.

Mice in the RT group were exposed to 16 Gy of radiation at a 600 Mu/min rate and were administered normal saline injections daily, equivalent to THD. In the RT+vehicle group, mice underwent the same radiation exposure, were injected with empty adenovirus, and were administered normal saline daily, equivalent to THD. For the RT+Th group, mice underwent the same radiation exposure and THD treatment via a daily intraperitoneal injection of 40 mg/mL THD (dimethylsulfoxide [DMSO] dissolution; dose, 100 mg/kg) for 7 days. In the RT+Th+si-NC group, mice received the same radiation exposure, were injected with LZTS3 negative plasmid packaged with adeno-associated virus AAV1, and were treated with THD daily (intraperitoneal injection, 40 mg/mL THD at a dose of 100 mg/kg) for 7 days. In the RT+Th+si-LZTS3 group, mice received the same radiation exposure, were injected with LZTS3 plasmid packaged with adeno-associated virus AAV1, and were treated with THD daily (intraperitoneal injection, 40 mg/mL THD at a dose of 100 mg/kg) for 7 days. Subsequently, all mice with fully damaged tongues were collected for further analysis 12 days later. All mice were killed by cervical dislocation.

Cell culture in a controlled environment, radiation, and transfection

We obtained and cultured human oral epithelial cell lines (HOEC, BeNa culture, 340217) in a humid environment at 37 °C with 5% CO₂, using a complete medium for human oral epithelial cells (CM-H203, Procell). There was no mycoplasma infection during cell culture, and the cells were transfected after two passes. To

facilitate transfection, HOECs were transfected with the LZTS3 overexpression plasmid (oeLZTS3), overexpression negative control (oeNC), small interfering RNA (siLZTS3) and small interfering RNA negative control (siNC). This process involved using Lipofectamine 6000 reagent (Thermo Fisher Scientific, Waltham, MA, USA) following the manufacturer's instruction. The RT+Th, RT+Th+OE-NC, and RT+Th+OE-LZTS3 groups were pre-treated with a 10 mg/mL THD solution (dissolved in DMSO) for 24 h. Subsequently, the medium was replaced in preparation for further experiments, and all the RT groups underwent radiotherapy with a 6 Gy dose for approximately 1.1 min.

RNA-sequencing

First, the cells were treated with radiation, THD was added to the experimental group, DMSO was added to the control group, and RNA of the cells was collected. Samples were evaluated using Agilent bioanalyzers. Sequencing was performed on the Illumina HiSeq2000 platform. RNA sequences were compared with hg38 using Bowtie2, and differential genes were analyzed using Dseq2 [17]. What is more, the RNA-seq data were list in Table S1.

Cell cycle analysis

For cell cycle analysis, the Cell cycle kit (C1052, Beyotime, Shanghai, China) is used. After the harvested cells were washed twice in PBS, they were added to 1 mL ice bath and pre-cooled in 70% ethanol, and fixed at 4 °C overnight. After washing twice in PBS, propyl iodide (PI) staining was performed, followed by flow cytometry (CytoFLEX; BECKMAN COULTER) analyzed the cell cycle and used ModFit LT 5.0 to determine the proportion of cells in each sample at each stage.

Hematoxylin and eosin (H&E) and Masson staining

Tongue tissues were fixed in 4% paraformaldehyde and then preserved in paraffin. Subsequently, 3 μm sections were prepared and stained with H&E and Masson's trichrome.

Cell counting Kit-8 (CCK-8) assay

The CCK-8 cytotoxicity assay required seeding cells in a 96-well plate with a clear bottom at a density of 2×10^4 cell/ml. The cells were treated according to the manufacturer's instructions (BS350B, Biosharp), and they were quantified using a multifunctional enzyme reader (Filter-Max F3, MD, USA).

Enzyme-linked immunosorbent assay (ELISA)

After washing the tongue tissues, the supernatant underwent homogenization and centrifugation at 4 °C at 2000 rpm for 20 min. Subsequently, we measured TNF-α,

IL-6, and IL-1a levels according to the instructions provided with the kit.

Reverse transcription-quantitative polymerase chain reaction (RT-qPCR)

TriQuick Reagent (R1100, Solarbio, Beijing, China) was utilized to extract total RNA following the manufacturer's guidelines. The template RNA was then reverse-transcribed and amplified using MonScript™ RTIIIAll-in-One Mix containing dsDNase (MR05101, Monad, Wuhan, China). Subsequently, we used the SYBR Green PCR Master Mix (11201ES03, Yeasen, Shanghai, China) and amplified the cDNA obtained using primers to assess mRNA expression. Appendix Table S2 lists the primers sequences for RT-qPCR.

Western blotting (WB)

We used 10–15% sodium dodecyl-sulfate polyacrylamide gel electrophoresis to evaluate equal amounts of total protein extracts obtained from cultured cells or tissues. These extracts were subsequently transferred onto polyvinylidene fluoride (PVDF) membranes. We employed primary antibodies targeting BAX, Bcl-2, caspase-3, and caspase-9. The extracts were then assessed with a suitable secondary antibody conjugated with horseradish peroxidase. Appendix Table S3 shows a list of the utilized antibodies. The results were standardized to β-actin as an internal reference, and protein expression levels were quantified using Image J.

Cell apoptosis analysis using flow cytometry assay

Cellular damage was assessed using fluorescein isothiocyanate (FITC)-annexin V/propidium iodide (PI) staining. Fluorescent signals were detected with FACScan (BECKMAN COULTER, CytoFLEX), and FlowJo was used to analyze cellular apoptosis. Early apoptotic cells were identified as annexin-V-FITC+/PI-, late apoptotic cells as annexin-V-FITC+/PI+, and necrotic cells as annexin-V-FITC-/PI+.

Immunohistochemical analysis

The obtained mouse tongue tissues were preserved with formalin and fixed with paraffin wax. The tissue was further cut to a thickness of 3 μm, baked overnight at 65 °C, dewaxed to water and then antigen repaired. Next, they were incubated at 3% H₂O₂ for 10 min, followed by exposure to anti-rat LZTS3 antibodies (1:400) and stored at 4 °C for 12 h. Finally, the slides were rinsed with PBS and exposed to biotinylated enzymic secondary antibody for 30 min. The slides treated with streptavidin biotin HRP complex were further treated with DAB chromogenic agent and stained with hematoxylin.

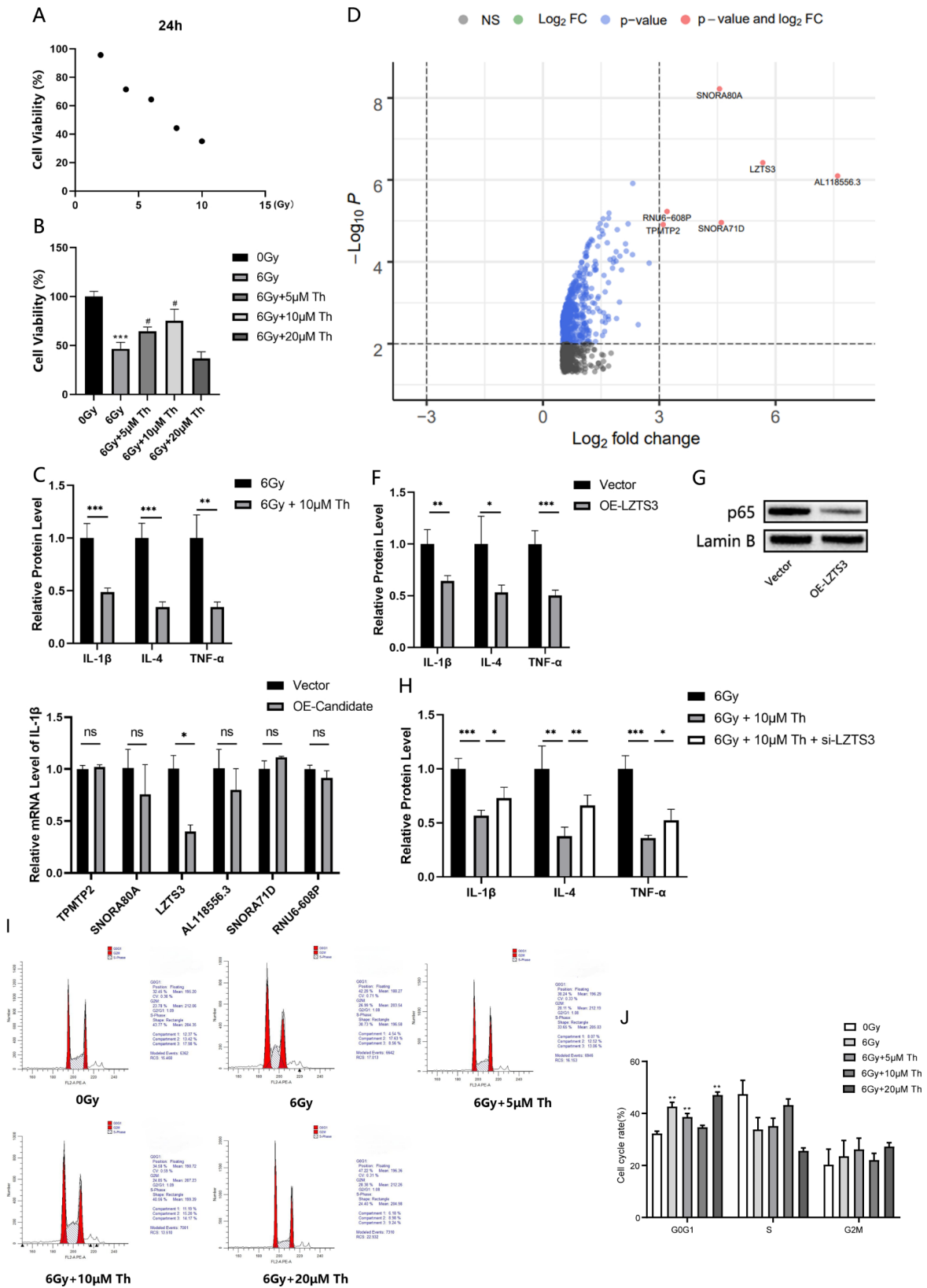


Fig. 1 (See legend on next page.)

(See figure on previous page.)

Fig. 1 LZTS3 is regulated by RT and THD. **(A)** Cell activity was measured by MTT assay, and the results showed the effect of different doses of X-ray irradiation on HOEC activity; **(B)** MTT assay was used to detect cell activity. After 6 Gy radiation, the results showed that thalidomide at 10 μ M concentration had the best recovery effect on cell activity; **(C)** ELISA results showed that thalidomide could effectively inhibit RIOM cell inflammatory factors; **(D)** The volcano map showed that the expression of differential genes increased in the RIOM cell model after the addition of thalidomide, Log₂FC > 0.5, $p < 0.05$ genes, and the six genes with the most obvious upregulation and statistical significance were highlighted in red (Log₂FC > 3, $p < 0.01$); **(E)** RT-qPCR results showed that the transcription level of IL-1 β in RIOM cell models decreased significantly after overexpression of LZTS3; **(F)** ELISA results showed that the IL-1 β , IL-4 and TNF- α released by cells were significantly decreased after overexpression of LZTS3; **(G)** WB results showed that the content of NF- κ B complex subunit p65 in the nucleus was significantly decreased after overexpression of LZTS3; **(H)** ELISA results showed that LZTS3 knockdown could restore thalidomide's inhibitory phenotype for inflammatory factors expression; **(I)** Cell cycle distribution under radiation and THD; **(J)** A statistical map of cell cycle distribution shows that radiation causes an increase in G0G1 phase cells. * $P < 0.05$, ** $P < 0.01$ and *** $P < 0.001$

Statistical analysis

Data are expressed using mean \pm standard deviation from a minimum of three distinct experiments. To assess the differences among various groups, a one-way analysis of variance (ANOVA) was conducted, followed by Tukey's test. The normality of the data distribution had been assessed before the parameter test was performed. Data between groups were compared using a t-test. Statistical analysis was conducted using SPSS v25.0, while charts were constructed using Prism v7.0. The outcome of the bilateral examination was considered statistically significant at a significance level < 0.05 .

Results

LZTS3 is regulated by RT and THD

We first examined the effects of radiation therapy on cell viability, and we set 5 time points and found that cell viability decreased with increasing radiation dose (Fig. 1A). We then added different concentrations of THD at a fixed radiation dose of 6 Gy, and found that THD could rescue the cell viability decline caused by radiotherapy in the concentration range of 0–10 μ M (Fig. 1B). Therefore, we determined the radiation dose of 6 Gy and 10 μ M THD as the criteria for follow-up experiments. In order to further test whether the addition of THD alleviated the inflammatory response of the cells, it was first found by Elisa that the addition of THD reduced the protein levels of IL-1 β , IL-4 and THF- α compared with the radiotherapy group (Fig. 1C). We conducted second-generation sequencing to explore the specific mechanism of THD regulating inflammation, and found that LZTS3, SON-RA80A, AL118556.3, SONA71D, TPMTP2, RNU6-608P and other genes were significantly up-regulated (Fig. 1D). Because IL-1 β is one of the most typical inflammatory agents, we verified the regulatory role of these genes on IL1- β . The results showed that IL-1 β levels were significantly down-regulated when LZTS3 was overexpressed (Fig. 1E). We chose LZTS3 as the main research target and found that overexpression of LZTS3 reduced IL-1 β through Elisa experiments. Protein levels of IL-4, THF- α (Fig. 1F), and LZTS3 also decreased protein expression of p65 in the nucleus (Fig. 1G), indicating that the addition of LZTS3 not only inhibited the downstream validator but also inhibited the activation of NF- κ B pathway,

leading to a decrease in the entry of P65 into the nucleus. When treated with radiotherapy combined with THD, LZTS3 knocking down attenuates the inhibitory effect of THD on inflammation (Fig. 1H). These results suggest that THD may influence the inflammatory response of cells by regulating LZTS3. We further explored the way THD protects cells by detecting cell cycle distribution (Fig. 1I). We found that when cells were exposed to a radiation dose of 6 Gy, G1S checkpoint tissues would occur, and more cells were distributed in the G0G1 phase. When 5–10 μ M of THD was added, the degree of cell damage was reduced. More cells entered the S phase through the G1S checkpoint, while 20 μ M of THD seemed to do the opposite (Fig. 1J).

LZTS3 inhibits HOEC apoptosis

To confirm the significance of LZTS3 in the protective effect of THD in RIOM, our subsequent analysis focused on exploring the involvement of LZTS3 in the apoptotic or inflammation cytokine function during the RIOM process. LZTS3 overexpression plasmid (oeLZTS3), empty overexpression control plasmid (oeNC), two LZTS3 small interfering RNAs (siLZTS3-1, siLZTS3-2), and empty knockout control small interfering RNA (siNC) were constructed. RT-qPCR (Fig. 2A) and WB (Fig. 2E) were used to assess the effectiveness of knockout and overexpression. The results showed that oeLZTS3 significantly increased LZTS3 expression, whereas siLZTS3-1 and siLZTS3-2 reduced NFATC2 expression in HOECs compared with their respective negative controls.

Bax and Bcl-2 are important regulators and markers of apoptosis. Bax promotes apoptosis, while Bcl-2 inhibits apoptosis. Based on the RT-qPCR and WB results (Fig. 2D), radiotherapy increased pro-apoptotic factor Bax expression while decreasing anti-apoptotic factor Bcl-2 expression at the mRNA and protein levels. Conversely, LZTS3 overexpression downregulated Bax (Fig. 2B, G) and upregulated Bcl-2 expression (Fig. 2C, F), while LZTS3 depletion upregulated Bax (Fig. 2B, G) and downregulated Bcl-2 expression (Fig. 2C, F). In addition, caspase-3 and caspase-9, two proteins that promote cell death, also showed change patterns similar to Bax (Fig. 2H, I), that is, they were down-regulated when LZTS3 was overexpressed and up-regulated when

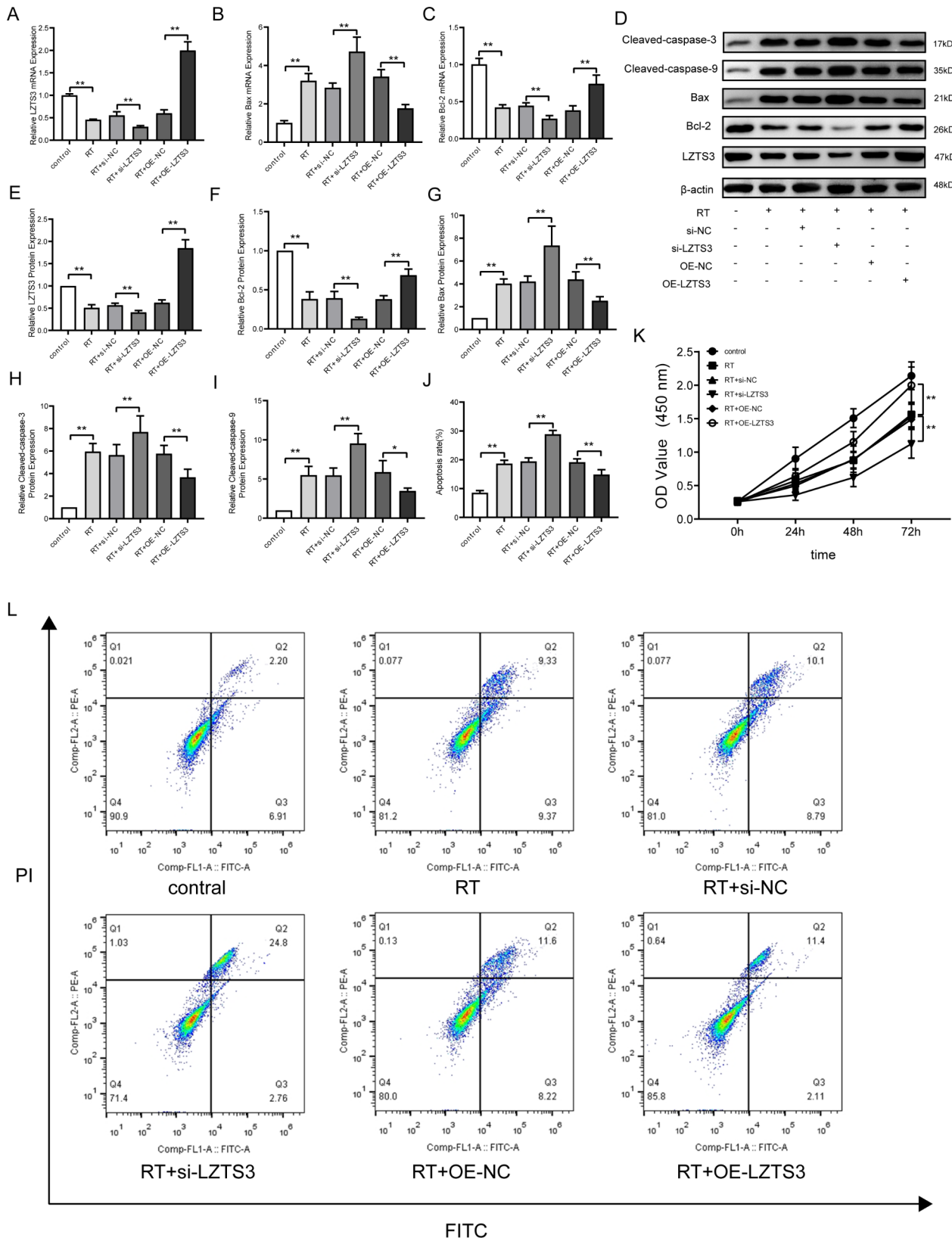


Fig. 2 LZTS3 promotes apoptosis in HOECs. mRNA expression levels of LZTS3 (A), Bax (B), and Bcl-2 (C). Apoptosis-associated protein expression was assessed using western blotting (WB). Protein expression of LZTS3 (E), Bcl-2 (F), Bax (G), caspase-3 (H), and caspase-9 (I). Evaluation of OD value at 450 nm using CCK-8 assay following transfection. Flow cytometry was used to determine the apoptosis ratios of HOECs after transfection (* $p < 0.05$, and ** $p < 0.01$)

LZTS3 was knocked down. In CCK-8, increased LZTS3 expression significantly promoted cell viability, while cell proliferation was reduced when LZTS3 was down-regulated (Fig. 2K). In addition, Annexin V-FITC/PI staining showed that increased expression of LZTS3 significantly reduced apoptosis of HOECs. On the contrary, apoptosis levels were significantly increased after LZTS3 inhibition (Fig. 2J, L). These results suggest that LZTS3 can protect cells from apoptosis.

LZTS3 inhibits pro-inflammatory cytokine production in HOECs

Subsequently, we investigated the role of LZTS3 in the inflammatory process. Inflammation is sustained by IL-1 α , IL-6, and TNF- α , enhancing vascular permeability and tissue edema, stimulating immune cells, and promoting inflammatory cell movement and attachment. Based on the RT-qPCR test results, radiotherapy led to increased mRNA levels of IL-1 α , IL-6, and TNF- α compared with the control. Additionally, LZTS3 knockdown further increased the mRNA expression of these inflammatory factors, while LZTS3 overexpression decreased the heightened expression of inflammatory factors induced by radiotherapy (Fig. 3A–C). The cell culture supernatants were then collected to assess inflammatory factors using ELISA. The results showed that decreasing the expression of LZTS3 increased the secretion of IL-1 α , IL-6 and TNF- α . Conversely, overexpression of LZTS3 reduced radiation-induced secretion of IL-1 α , IL-6, and TNF- α (Fig. 3D–F). Phosphorylation enhances NF- κ B p65 translocation into the nucleus, thereby increasing its ability to regulate gene expression through transcriptional activity. p-NF- κ B p65 is vital in inflammation and immune responses. The WB test revealed that radiotherapy and LZTS3 had no significant effect on NF- κ B p65 expression. However, both radiotherapy and LZTS3 knockdown significantly enhanced NF- κ B p65 phosphorylation. In contrast, overexpression of LZTS3 leads to reduced phosphorylation of NF- κ B p65 and reduced translocation of NF- κ B p65 into the nucleus (Fig. 3G–I).

THD reduces cell apoptosis induced by radiation

To investigate the effect of THD on cell death and its relationship with LZTS3, we introduced 10 μ M THD to the cellular environment. To further investigate the effect of THD on apoptosis and inflammation while inhibiting LZTS3 expression. The PCR findings indicated that THD introduction following radiotherapy resulted in LZTS3 and Bcl-2 mRNA upregulation, while Bax down-regulation was observed (Fig. 4A–C), thereby exerting an anti-apoptotic function. This anti-apoptotic effect was reversed by LZTS3 knockdown. Consistent results were also observed in WB experiments (Fig. 4D). At the protein level, THD presence caused a upregulation in LZTS3

protein levels, followed by an increase in Bcl-2 expression and a decrease in Bax, caspase-3, and caspase-9 protein expression levels. Consequently, this had an anti-apoptotic effect. Conversely, when LZTS3 was knocked down, Bax, caspase-3, and caspase-9 were upregulated, and Bcl-2 was downregulated, cells exhibit a propensity towards apoptosis (Fig. 4E–G). This indicates that THD exerts an anti-apoptotic function by upregulating LZTS3 expression. In the CCK-8 experiment, cell proliferation was significantly increased after the introduction of THD after radiotherapy, and cell viability was significantly decreased after LZTS3 knockdown (Fig. 4K). Annexin V-FITC/PI staining revealed that THD substantially suppressed apoptosis in HOEC. Conversely, the THD-induced reduction in apoptosis was reversed by LZTS3 knockdown (Fig. 4J, L). These results suggest that THD protects cells from apoptosis by up-regulating LZTS3, and down-regulating LZTS3 can reverse this protective effect.

THD reduces inflammation in HOECs

We further assessed the role and mechanism of THD and LZTS3 in inflammatory responses. The results showed that THD introduction to cells caused a significant decrease in the mRNA expression of IL-1 α , IL-6, and TNF- α , which mitigated the inflammatory response. However, the reduction of LZTS3 caused an increase in the levels of the inflammatory factors that had previously decreased (Fig. 5A–C), as indicated by the RT-qPCR results. Simultaneously, we measured IL-1 α , IL-6, and TNF- α concentrations in the cell culture supernatant using ELISA. THD reduces these levels, and with LZTS3 knocked down THD loses its ability to down-regulate inflammatory cytokines (Fig. 5D–F). The WB experiment showed that THD introduction following radiotherapy had no significant effect on NF- κ B p65 protein expression (Fig. 5G, H). However, it significantly reduced p-NF- κ B p65 expression levels, thereby affecting the nuclear entry of NF- κ B p65. Knockdown of LZTS3 promoted NF- κ B p65 phosphorylation, effectively attenuating the influence of THD (Fig. 5I). The findings indicate that THD can effectively reduce inflammatory marker expression by targeting LZTS3.

THD pretreatment protects irradiated mice from mucositis

To further confirm our findings in vivo, we constructed an irradiated mouse model and collected tongue tissue samples for subsequent experimental analysis. We first used immunohistochemistry to detect the expression of LZTS3 protein in different groups (Fig. 6A), and we found the same trend as in the previous in vitro experiment. Compared with the control group, radiotherapy with 6 Gy resulted in the decrease of LZTS3, while the addition of THD could partially recover the downregulation

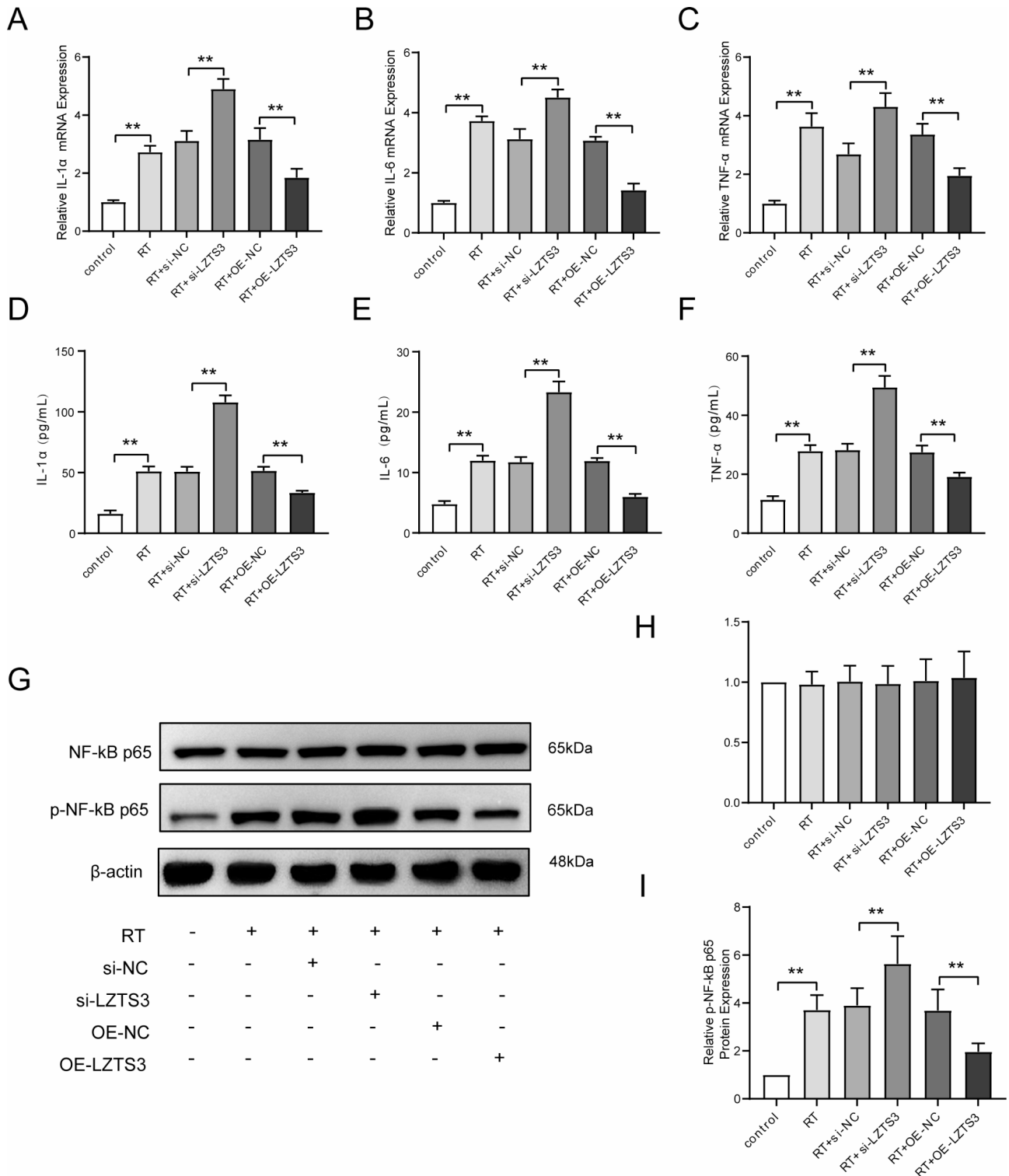


Fig. 3 LZTS3 enhances the production of inflammatory cytokines in HOECs. Expression levels of IL-1α (A), IL-6 (B), and TNF-α (C) mRNA. ELISA was used to assess the protein expression levels of IL-1α (D), IL-6 (E), and TNF-α (F). WB was used to detect protein expression levels associated with inflammation (G), including NF-κB p65 (H) and p-NF-κB p65 (I). (* $p < 0.05$, and ** $p < 0.01$)

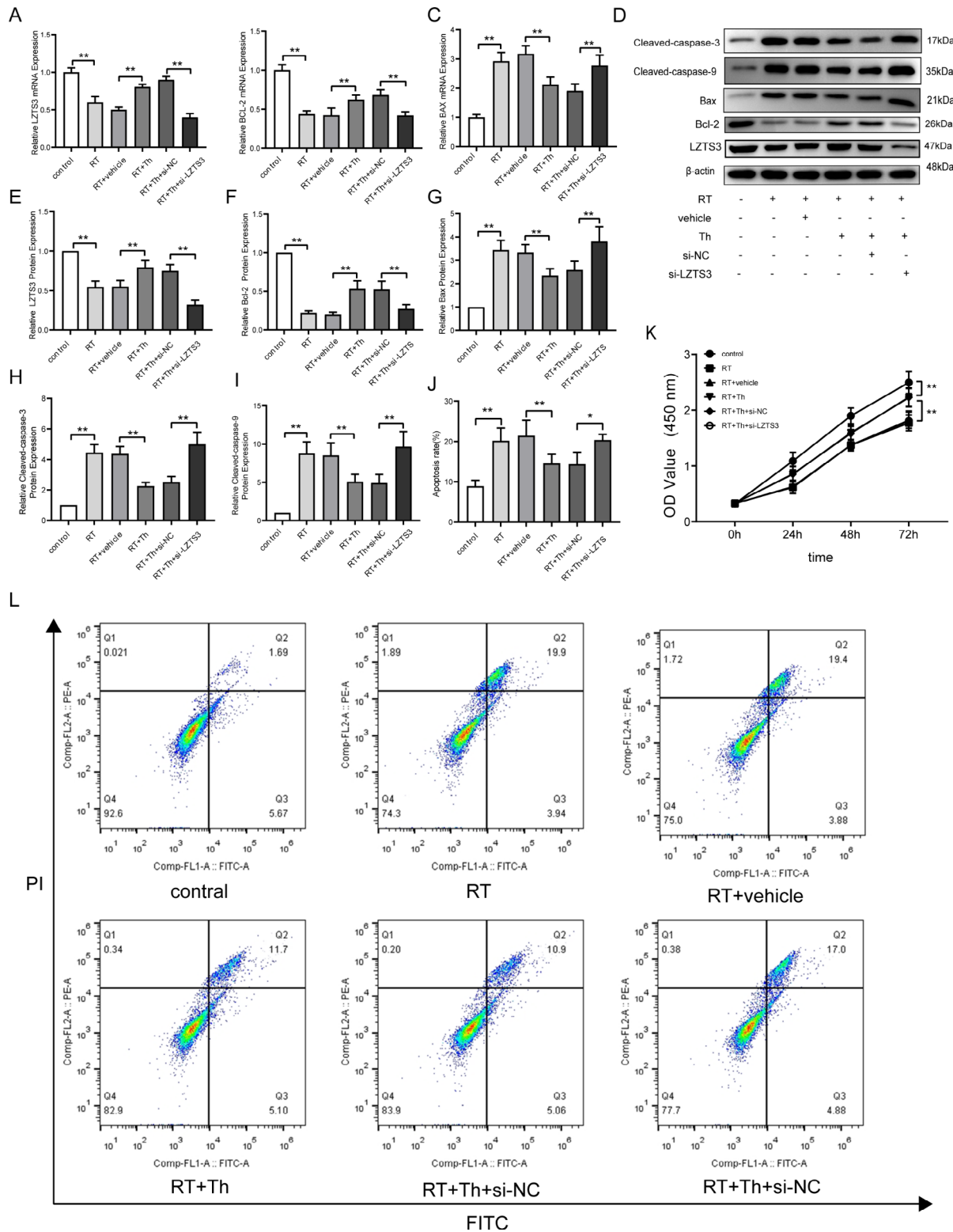


Fig. 4 THD decreased radiation-induced cell apoptosis. mRNA expression levels of LZTS3 (A), Bcl-2 (B), and Bax (C). Apoptosis-associated protein expression was assessed using western blotting (WB) (D). Protein expression of LZTS3 (E), Bcl-2 (F), Bax (G), caspase-3 (H), and caspase-9 (I). Evaluation of OD value at 450 nm using CCK-8 assay following transfection (K). Flow cytometry (L) was used to measure the apoptosis ratios of HOECs after transfection ($n=3$, $*p<0.05$, and $**p<0.01$). Between different groups after radiotherapy, apoptosis rate and the introduction of THD relationship (J). ($*p<0.05$, and $**p<0.01$)

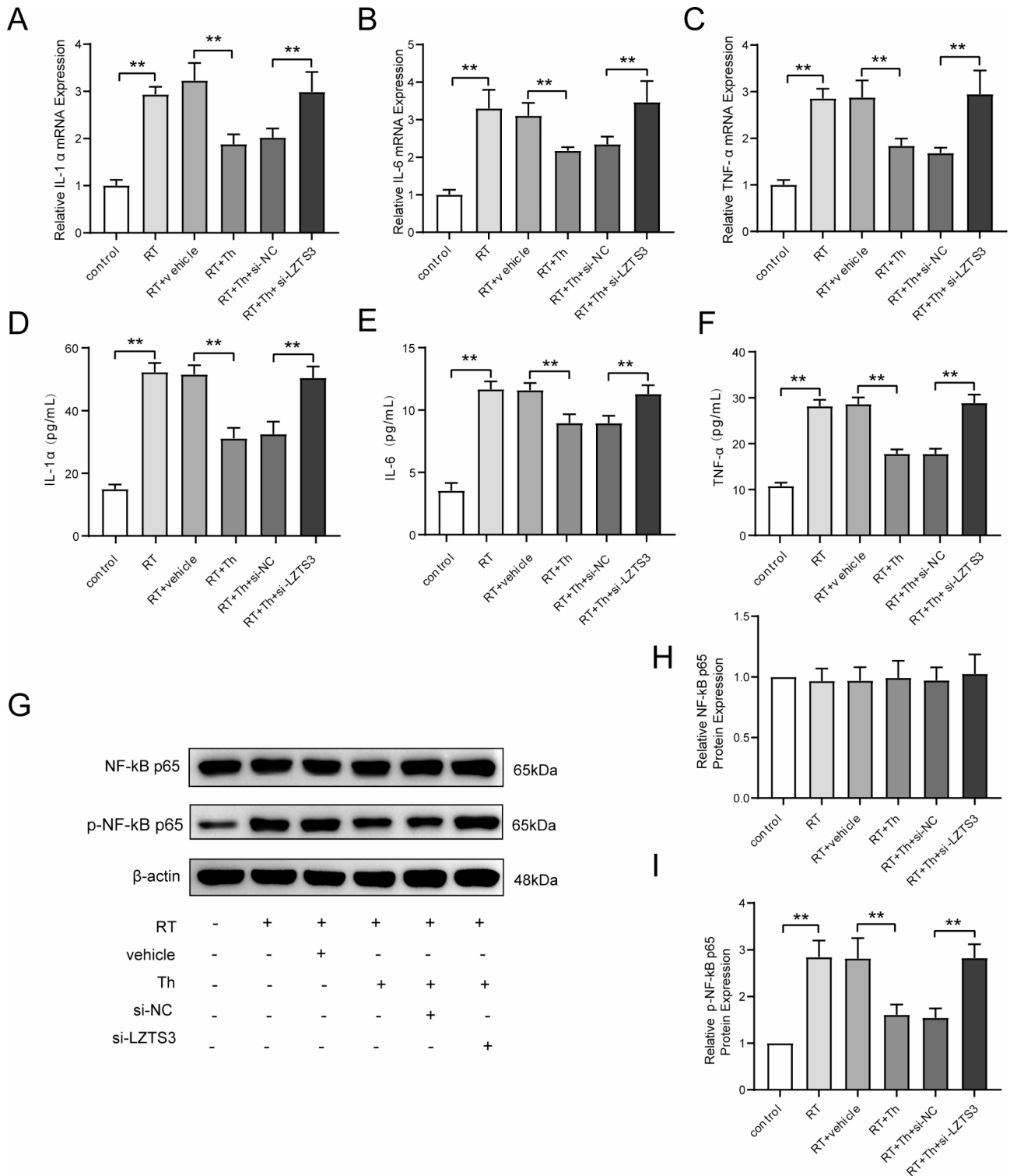


Fig. 5 THD decreases inflammation in HOECs. Expression levels of IL-1α (A), IL-6 (B), and TNF-α (C) mRNA. ELISA was used to assess IL-1α (D), IL-6 (E), and TNF-α (F) protein expression levels. WB analysis (G) was performed to determine protein expression levels associated with inflammation, specifically of NF-κB p65 (H) and p-NF-κB p65 (I). (**p* < 0.05, and ***p* < 0.01)

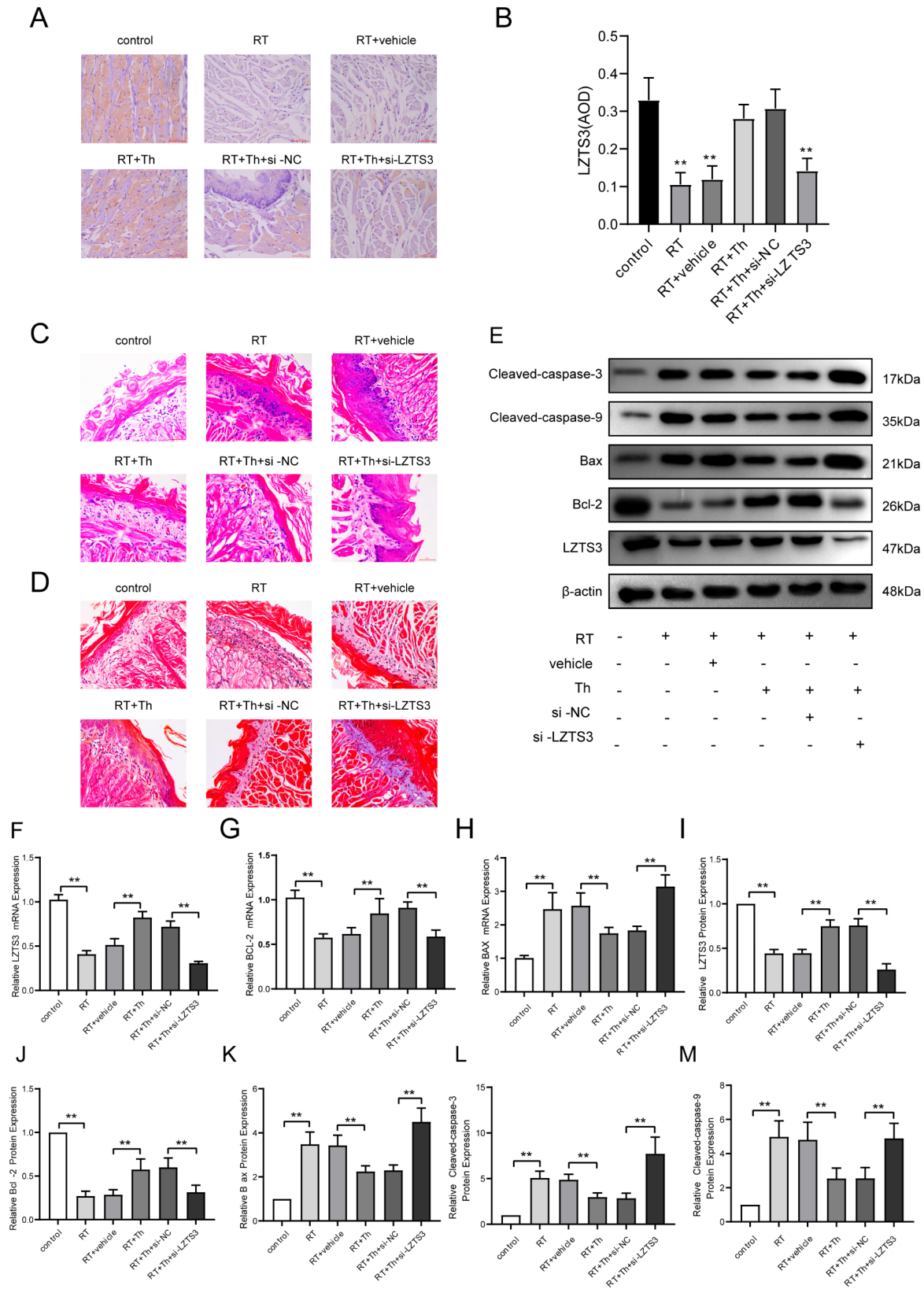


Fig. 6 THD inhibits apoptosis by downregulating LZTS3 in irradiated mice. **(A)** Immunohistochemical staining of LZTS3; **(B)** Statistical diagram of staining intensity of LZTS3; H&E staining **(C)** and Masson staining **(D)** of the tongue tissue. mRNA expression levels of LZTS3 **(F)**, Bax **(G)**, and Bcl-2 **(H)**. Protein expression of LZTS3 **(I)**, Bcl-2 **(J)**, Bax **(K)**, caspase-3 **(L)**, and caspase-9 **(M)** was analyzed using western blotting **(E)**. (* $p < 0.05$, and ** $p < 0.01$)

of LZTS3 caused by radiotherapy (Fig. 6B). H&E staining, a conventional technique, is primarily used to observe the structural characteristics of cell nuclei and cytoplasm in tissues. The H&E staining results revealed that the basal cell layer in the RT and RT+vehicle groups exhibited a significant increase in thickness than that of the control group. Additionally, epithelial cell arrangement disruption and inflammatory cell infiltration occurred in the mucous lamina propria. Conversely, the basal membrane in the RT+Th and RT+Th+si-NC groups remained intact. However, in the RT+Th+si-LZTS3 group, a significant increase in the basal cell layer thickness was observed, along with a substantial infiltration of inflammatory cells in the mucous lamina propria. Additionally, epithelial cell arrangement was disrupted (Fig. 6C).

Masson staining is a specialized method primarily used to observe collagen and muscle fiber distribution. The results showed the following: in the control group, the tongue anatomy was within the expected range; the RT and RT+vehicle groups exhibited an increase in collagen and elastic fibers compared with the control group; the control group showed no significant variations in collagen and elastic fibers compared with the RT+Th and RT+Th+si-NC groups; in the RT+Th+si-LZTS3 group, collagen fibers were significantly thick, dense, and closely arranged, with varying thicknesses. Furthermore, a significant increase in collagen fibers was observed, resulting in a more intense staining than that of the control group (Fig. 6D).

These findings suggest that radiation exposure can lead to tissue structure disturbances, thickening of the basal cell layer, inflammatory cell infiltration, and increased collagen and elastic fibers, while the addition of THD can protect tissues by upregulating LZTS3. To enhance the credibility of our findings, we constructed an irradiated mouse model and validated the conclusions derived from our cellular experiments *in vivo*. We specifically demonstrated that THD downregulated LZTS3 expression, thereby inhibiting the release of pro-inflammatory factors and cell apoptosis. To substantiate our findings, we obtained mouse tongue tissue samples and performed WB analysis. The findings indicated that, compared with that of control mice, the tongue tissue of the irradiated mice exhibited increased LZTS3, BAX, caspase-3, and caspase-9 expression, whereas BCL-2 expression was decreased (Fig. 6E, I–M). The introduction of THD can counteract this trend by decreasing the expression of LZTS3, and when LZTS3 is knocked down, the anti-apoptotic and anti-inflammatory effects of THD are cancelled out. PCR was used to detect LZTS3, BAX, and BCL-2 mRNA expression, and the tendency of the results were consistent with results of WB (Fig. 6F–H).

Additionally, inhibiting LZTS3 with THD can effectively mitigate the inflammatory response in tissues. In

our PCR experiment, the addition of THD inhibited the increase in the levels of radiation-induced inflammatory cytokines, such as IL-1 α , IL-6 and TNF- α , while the addition of THD accompanied by knockdown of LZTS3 reversed the inhibitory effect of THD on inflammation (Fig. 7A–C). These findings were consistent with the ELISA results (Fig. 7D–F). Additionally, the WB experiment showed that THD could reduce NF- κ B p65 phosphorylation by upregulating LZTS3 (Fig. 7G–I). These *in vivo* experimental results further proved that THD inhibits the release of inflammatory factors by elevating LZTS3, which is a necessary downstream role of THD. When LZTS3 is knocked down, the role of THD cannot be played.

Discussion

Radiation oral mucositis (RIOM), as a common oral complication, occurs in individuals who are treated with radiotherapy or radiation for head and neck tumors. It greatly affects the quality of life and prognosis of patients. There are many ways to intervene, but there is no acknowledged standard treatment for preventing RIOM. Reducing the prescribed radiotherapy dose led to a decrease in the occurrence and severity of mucositis. This reduction in the total prescribed dose significantly lowers the incidence of grade III or higher RIOM occurrence [18, 19]. However, healthcare providers should approach treatment strategies with caution to avoid compromising effectiveness while reducing the dosage. Moreover, specific anti-inflammatory medications, including benzydamine, have been proven to prevent RIOM and decrease its intensity when applied in randomized controlled trials. Furthermore, medications, including celecoxib, misoprostol, and rebapenem, have demonstrated effectiveness in limited research, although evidence supporting their usage is insufficient [20]. Avasopasem manganese (GC4419), a novel treatment, can help reduce G3 RIOM severity and duration. However, its administration via intravenous infusion for >1 h presents challenges in medical settings [21]. Researchers have long strived for the safety and effective control of RIOM.

Our preliminary clinical trials confirmed the efficacy and safety of THD in preventing RIOM, suggesting that this is a promising therapeutic drug [13]. Limited evidence suggests that cellular inflammation and apoptosis are critical in the progression of RIOM, with TNF- α , prostaglandin, NF- κ B, and IL-1 β showing strong correlations in radiotherapy-induced mucosal damage. Therefore, we further explore the specific mechanism of THD in preventing RIOM here. In this study, LZTS3 was experimentally identified as a key factor in the control and treatment of RIOM by THD. Promoting LZTS3 with THD prevented RIOM, offering substantial support for treating this condition. LZTS3 was first identified in

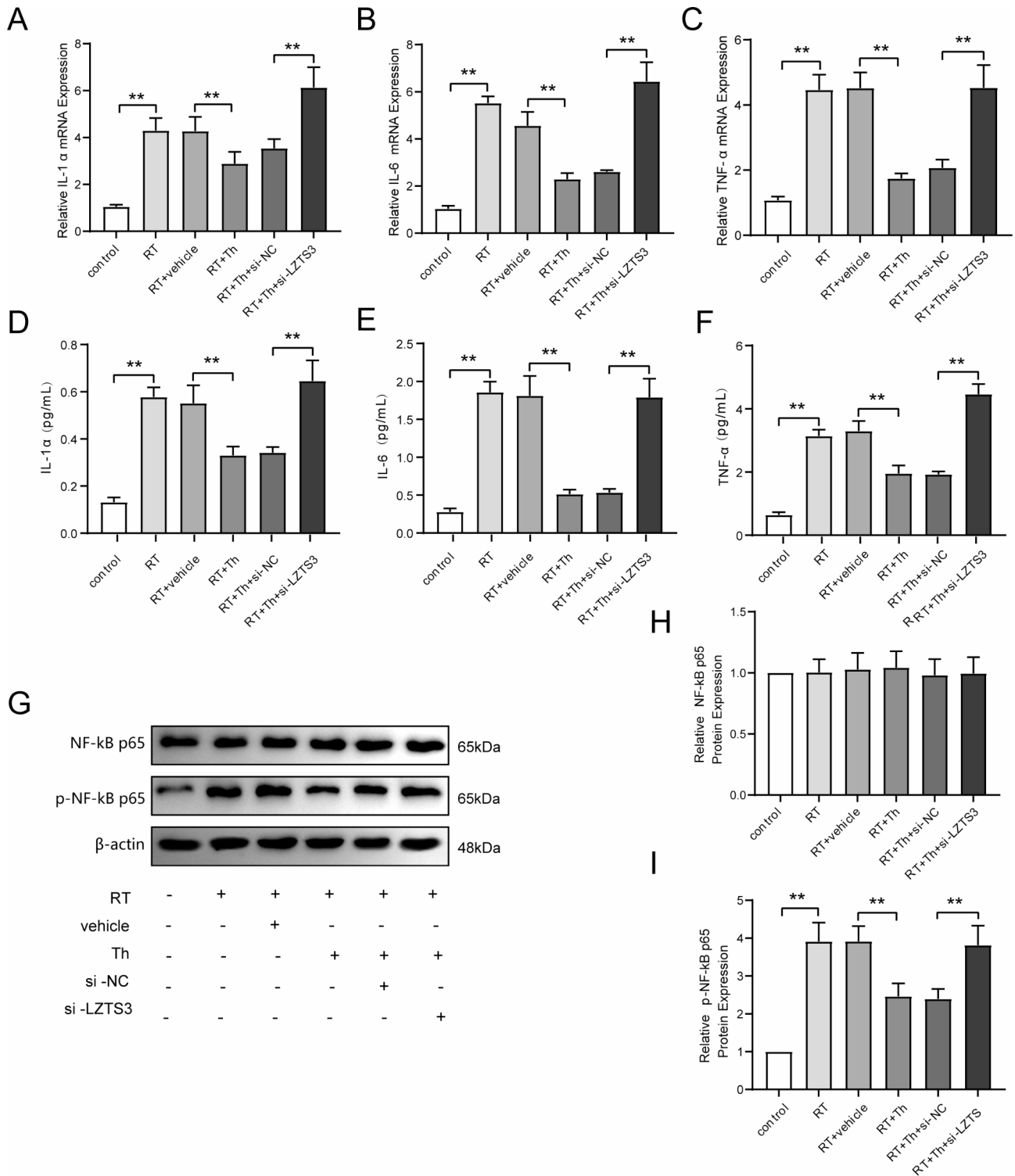


Fig. 7 THD reduces inflammation in irradiated mice. Expression levels of IL-1α (A), IL-6 (B), and TNF-α (C) mRNA. ELISA was used to assess IL-1α (D), IL-6 (E), and TNF-α (F) protein expression levels. WB analysis (G) was performed to determine protein expression levels associated with inflammation, specifically NF-κB p65 (H) and p-NF-κB p65 (I). (**p* < 0.05, and ***p* < 0.01)

2005 and belongs to the leucine zipper tumor suppressors (LZTS) protein family [16]. LZTS3 has been shown to inhibit tumor progression in colorectal adenocarcinoma and lung cancer [22, 23]. Additionally, bioinformatics studies have associated LZTS3 with colon cancer prognosis [24] and Parkinson's disease. However, to the best of our knowledge, no reports on LZTS3 involvement in RIOM exist. The findings of this study, for the first time, reveal that LZTS3 can inhibit apoptosis and pro-inflammatory cytokine secretion in RIOM. Furthermore, this study elucidated the mechanism by which THD can effectively treat RIOM by evaluating LZTS3 levels, thereby providing further support for its clinical utilization. By regulating the LZTS3 levels, LZTS3 was observed to inhibit pro-inflammatory molecule secretion, including IL-1 α , IL-6, and TNF- α , and influence NF- κ B-p65 phosphorylation. Additionally, LZTS3 could influence apoptosis by affecting Bax, Bcl-2, caspase-3, and caspase-9. To inhibit the radiation-induced downregulation of LZTS3, THD up-regulate LZTS3 expression at the transcriptional and protein levels, consequently mitigating apoptosis and pro-inflammatory factor release. Our findings were validated, as THD effectively inhibited apoptosis and inflammation by upregulating LZTS3 expression in an irradiated mouse model. However, this study has some limitations. First, our sequencing data originated from processed cell lines, which may differ from clinical samples. Second, RIOM pathogenesis differs significantly across various stages, making it uncertain at which stage THD contributes. Thirdly, We should further explore the combined application of thalidomide with other therapeutic methods such as immunotherapy, targeted therapy, etc., and further verify the difference in efficacy through experimental data.

In conclusion, this study identified the downstream acting factor LZTS3 that THD plays a therapeutic role in RIOM. LZTS3 can inhibit cell apoptosis and the release of inflammatory factors, and THD plays a protective role by up-regulating LZTS3. This lays a solid foundation for the medical application of THD and provides a potential target for the future treatment of RIOM.

Supplementary Information

The online version contains supplementary material available at <https://doi.org/10.1186/s12967-024-05648-z>.

Supplementary Material 1

Authors Contribution

Z.L. and J.Z. conceived and supervised the study. Z.L., L.L., M.G. and H.M. designed and performed the experiments. L.L., M.G., H.M. and J.L. analyzed the data. J.L. and C.L. drafted the manuscript. J.Q., K.R. and H.Z. provided insightful suggestions and experimental materials. All authors read and approved the final manuscript.

Funding

This study was supported by grants from the National Natural Science Foundation of China (82260627 and 82260604).

Data availability

Data will be available on reasonable request.

Declarations

Ethics approval

I promise that the study was performed according to the international, national and institutional rules considering animal experiments, clinical studies and biodiversity rights. The study protocol was approved by the Guangxi Medical University.

Conflict of interest

The authors declare that they have no competing interests.

Author details

¹Department of Oncology, The Sixth Affiliated Hospital of Guangxi Medical University, The First People's Hospital of Yulin, Yulin 537000, Guangxi, China

²Department of Colorectal Surgery, Cancer Hospital of Dalian University of Technology, Cancer Hospital of China Medical University, Liaoning Cancer Hospital & Institute, Shenyang 110042, Liaoning, China

³China Medical University, Shenyang 110000, Liaoning, China

⁴Department of Pharmacy, The Sixth Affiliated Hospital of Guangxi Medical University, The First People's Hospital of Yulin, Yulin 537000, Guangxi, China

⁵Department of Clinical Laboratory, The Sixth Affiliated Hospital of Guangxi Medical University, The First People's Hospital of Yulin, Yulin 537000, Guangxi, China

⁶Otolaryngology Head and Neck Surgery, The Sixth Affiliated Hospital of Guangxi Medical University, The First People's Hospital of Yulin, Yulin 537000, Guangxi, China

⁷Department of Oncology, The First Affiliated Hospital of Gannan Medical University, Ganzhou 341000, Jiangxi, China

Received: 18 July 2024 / Accepted: 12 September 2024

Published online: 27 September 2024

References

1. Elad S, Yarom N, Zadik Y, Kuten-Shorrer M, Sonis ST. The broadening scope of oral mucositis and oral ulcerative mucosal toxicities of anticancer therapies. *Cancer J Clin.* 2022;72:57–77.
2. Muanza TM, Cotrim AP, McAuliffe M, Sowers AL, Baum BJ, Cook JA, et al. Evaluation of radiation-induced oral mucositis by optical coherence tomography. *Clin cancer Research: Official J Am Association Cancer Res.* 2005;11:5121–7.
3. Elting LS, Cooksley CD, Chambers MS, Garden AS. Risk, outcomes, and costs of radiation-induced oral mucositis among patients with head-and-neck malignancies. *Int J Radiat Oncol Biol Phys.* 2007;68:1110–20.
4. Thomsen M, Vitetta L. Adjunctive treatments for the prevention of chemotherapy- and radiotherapy-induced mucositis. *Integr cancer Ther.* 2018;17:1027–47.
5. Chen C, Zhang Q, Yu W, Chang B, Le AD. Oral mucositis: an update on innate immunity and new interventional targets. *J Dent Res.* 2020;99:1122–30.
6. Al-Ansari S, Zechara JA, Barasch A, de Lange J, Rozema FR, Raber-Durlacher JE. Oral mucositis induced by anticancer therapies. *Curr oral Health Rep.* 2015;2:202–11.
7. Sonis ST. The pathobiology of mucositis. *Nat Rev Cancer.* 2004;4:277–84.
8. Köstler WJ, Hejna M, Wenzel C, Zielinski CC. Oral mucositis complicating chemotherapy and/or radiotherapy: options for prevention and treatment. *Cancer J Clin.* 2001;51:290–315.
9. Sonis ST. Mucositis as a biological process: a new hypothesis for the development of chemotherapy-induced stomatotoxicity. *Oral Oncol.* 1998;34:39–43.
10. Feller L, Essop R, Wood NH, Khammissa RA, Chikte UM, Meyerov R, et al. Chemotherapy- and radiotherapy-induced oral mucositis: pathobiology, epidemiology and management. *SADJ: J South Afr Dent Association = Tydskrif Van die Suid-Afrikaanse Tandheelkundige Vereniging.* 2010;65:372–4.

11. Chen M, Xie H, Chen Z, Xu S, Wang B, Peng Q, et al. Thalidomide ameliorates rosacea-like skin inflammation and suppresses NF- κ B activation in keratinocytes. *Biomed Pharmacother*. 2019;116:109011.
12. Song T, Ma X, Gu K, Yang Y, Yang L, Ma P, et al. Thalidomide represses inflammatory response and reduces radiculopathic pain by inhibiting IRAK-1 and NF- κ B/p38/JNK signaling. *J Neuroimmunol*. 2016;290:1–8.
13. Harte MC, Saunbury TA, Hodgson TA. Thalidomide use in the management of oromucosal disease: a 10-year review of safety and efficacy in 12 patients. *Oral surgery, oral medicine, oral pathology and oral radiology*. 2020;130:398–401.
14. Frings K, Gruber S, Kuess P, Kleiter M, Dörr W, et al. Modulation of radiation-induced oral mucositis by thalidomide: preclinical studies. *Strahlentherapie Und Onkologie : Organ Der Deutschen Röntgengesellschaft*. 2016;192:561–8.
15. Liang L, Liu Z, Zhu H, Wang H, Wei Y, Ning X, et al. Efficacy and safety of thalidomide in preventing oral mucositis in patients with nasopharyngeal carcinoma undergoing concurrent chemoradiotherapy: a multicenter, open-label, randomized controlled trial. *Cancer*. 2022;128:1467–74.
16. Teufel A, Weinmann A, Galle PR, Lohse AW. In silico characterization of LZTS3, a potential tumor suppressor. *Oncol Rep*. 2005;14:547–51.
17. Love MI, Huber W, Anders S. Moderated estimation of fold change and dispersion for RNA-seq data with DESeq2. *Genome Biol*. 2014;15:550.
18. Dean JA, Welsh LC, Wong KH, Aleksic A, Dunne E, Islam MR et al. Normal tissue complication probability (NTCP) modelling of severe acute mucositis using a novel oral mucosal surface organ at risk. *Clinical oncology (Royal College of Radiologists (Great Britain))*. 2017;29:263–73.
19. Brodin NP, Kabarriti R, Garg MK, Guha C, Tomé WA. Systematic review of normal tissue complication models relevant to standard fractionation radiation therapy of the head and neck region published after the QUANTEC reports. *Int J Radiat Oncol Biol Phys*. 2018;100:391–407.
20. Elad S, Cheng KKF, Lalla RV, Yarom N, Hong C, Logan RM, et al. MASCC/ISOO clinical practice guidelines for the management of mucositis secondary to cancer therapy. *Cancer*. 2020;126:4423–31.
21. Anderson CM, Lee CM, Saunders DP, Curtis A, Dunlap N, Nangia C, et al. Phase IIb, randomized, double-blind trial of GC4419 versus placebo to reduce severe oral mucositis due to concurrent radiotherapy and cisplatin for head and neck cancer. *J Clin Oncology: Official J Am Soc Clin Oncol*. 2019;37:3256–65.
22. Feng J, Li J, Qie P, Li Z, Xu Y, Tian Z. Long non-coding RNA (lncRNA) PGM5P4-AS1 inhibits lung cancer progression by up-regulating leucine zipper tumor suppressor (LZTS3) through sponging microRNA miR-1275. *Bioengineered*. 2021;12:196–207.
23. Gu X, Chen S, Wang Z, Bu Q, An S. LZTS3/TAGLN suppresses cancer progression in human colorectal adenocarcinoma through regulating cell proliferation, migration, and actin cytoskeleton. *Arch Med Res*. 2023;54:102894.
24. Liu X, Bing Z, Wu J, Zhang J, Zhou W, Ni M, et al. Integrative gene expression profiling analysis to investigate potential prognostic biomarkers for colorectal cancer. *Med Sci Monitor: Int Med J Experimental Clin Res*. 2020;26:e918906.

Publisher's note

Springer Nature remains neutral with regard to jurisdictional claims in published maps and institutional affiliations.